European Polymer Journal 104 (2018) 99–105

Contents lists available at ScienceDirect

European Polymer Journal

journal homepage: www.elsevier.com/locate/europolj

Tunable wrinkle structure formed on surface of polydimethylsiloxane microspheres

Shaodi Zheng[a], Shilin Huang[b], Lian Xiong[a], Wei Yang[a], Zhengying Liu[a,*], Banghu Xie[a], Mingbo Yang[a]

[a] College of Polymer Science and Engineering, Sichuan University, Chengdu 610065, China
[b] School of Materials Science and Engineering, Sun Yat-sen University, Guangzhou 510275, China

ARTICLE INFO

Keywords:
PDMS microspheres
Wrinkling
Tunable surfaces

ABSTRACT

Soft materials with controlled surface patterns are useful for a range of applications, including microdevices, sensors and adhesives. In this work, the spontaneously wrinkled morphologies on the surfaces of crosslinked polydimethylsiloxane (PDMS) microspheres were observed. These wrinkled microspheres may have great potentials for construction of high-performance functional materials. They were fabricated in curable PDMS/water emulsions stabilized by surfactants. After curing and drying, the PDMS droplets in the emulsions formed microspheres with different surface wrinkling morphologies, including dimples and labyrinth patterns. The buckling patterns could be well tuned by the surfactant concentration, curing temperature, evaporation and compositions of PDMS phase. A power-law dependence of the wrinkling wavelength on microsphere radius was also observed. Furthermore, the wrinkling morphologies showed good reversibility by simply drying after wetting with water. It is speculated that the evaporation of dissolved water in the PDMS phase triggers interfacial instabilities and result in the wrinkled morphologies. This work gives new insights into the surface wrinkling behavior of soft microspheres, and provides a simple, efficient and environmentally friendly route to fabricate microspheres with complex surface patterns.

1. Introduction

Polymeric systems which can form patterns with controllable size, order, morphology, and complexity, have attracted increasing attentions because of a wide range of potential applications, such as sensors [1], microfluidic devices [2], responsive coatings [3–5], microlens arrays [6], optoelectronic devices [7–9] and a metrology for measuring mechanical properties of ultrathin films [10,11]. The wrinkling (or buckling) patterns are typically observed in bilayer systems consisting of thin films on compliant substrates. When the bilayer films were expanded thermally, mechanically or osmotically, the modulus mismatch between the bilayers creates compressive stresses that trigger buckling of the thin films, leading to the formation of wrinkling patterns. [12] The morphology, order, and complexity of the wrinkling patterns can be controlled by varying the physical properties and dimensions of the substrates and thin films in bilayer systems [13].

In nature, many surface wrinkling phenomena happen on non-planar substrates, e.g., the human skin, the dehydrated fruits and vegetables [14,15]. Owing to geometric constraints, surface wrinkling on curved surfaces can be quite different from those on planar surfaces [15–19]. Spherical surface has been widely used as a model system to study non-planar wrinkling both theoretically and experimentally [17–22]. In general, surface wrinkling patterns can be synthesized by various methods, such as UV irradiation and followed by solvent swelling [23,24], specific host–guest chemistry [10], and surface chemical oxidation by acid solution [25]. For instance, Breid et al. [24] explored surface wrinkling on PDMS caps. By ultraviolet/ozone (UVO) treatment, a stiff surface oxide layer was generated on the PDMS spherical caps. Swelling of this surface layer with ethanol vapor resulted in the formation of wrinkling patterns on the PDMS spherical caps. These wrinkling patterns easily disappeared upon solvent evaporation. Recently, Yin et al. [25] fabricated microspheres with wrinkling surfaces based on surface chemical oxidation of aqueous-phase-synthesized PDMS microspheres in a mixed $H_2SO_4/HNO_3/H_2O$ solution. This simple and high-output method generated stiff oxidized shells on the PDMS microspheres which were requisite for the surface wrinkling. Inspired by this, the wrinkled microspheres were obtained via constructing the unstable interface on the microspheres in this work.

Here, we report a simple method to fabricate PDMS microspheres

* Corresponding author.
E-mail address: liuzhying@scu.edu.cn (Z. Liu).

https://doi.org/10.1016/j.eurpolymj.2018.05.007
Received 12 February 2018; Received in revised form 30 April 2018; Accepted 8 May 2018
Available online 09 May 2018

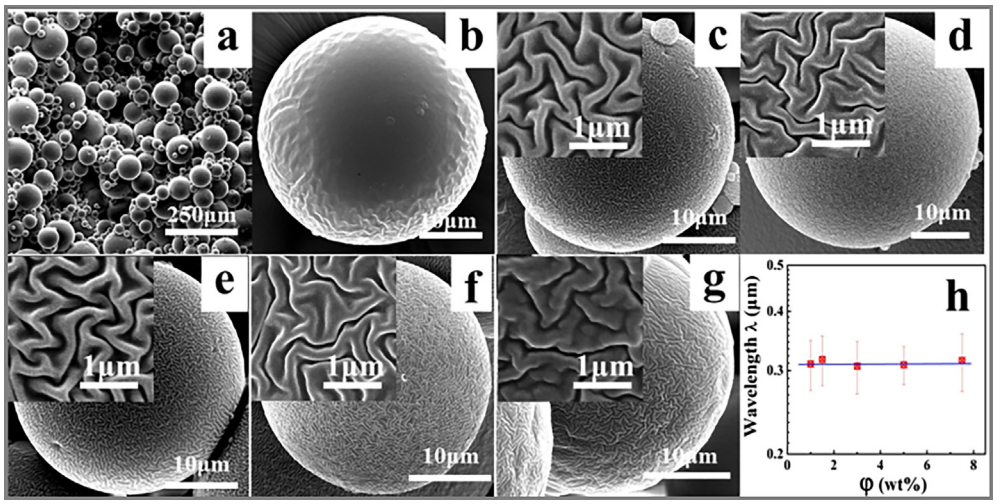

Fig. 1. (a) The overall view of polydisperse microspheres with 3 wt% surfactant and the $PDMS_{(10:1)}$ from SEM. Detailed SEM images of microspheres with $PDMS_{(10:1)}$ and various surfactant concentrations: (b) 0.7 wt%, (c) 1.0 wt%, (d) 1.5 wt%, (e) 3.0 wt%,(f) 5.0 wt%, (g) 7.5 wt%. (Inset) At higher magnification. Frame h showed the $\lambda \sim \varphi$ relationship for $PDMS_{(10:1)}$ microspheres of radius around 20 μm.

with labyrinth and buckyball-like surface patterns from a conventional oil/water emulsion stabilized by surfactants. The wrinkling patterns could be well tuned by modifying the experimental conditions such as the surfactant concentration, curing temperature, evaporation rate and weight ratio of base/curing agent. To the best of our knowledge, this is the first time report to realize surface wrinkling on the PDMS microspheres without any surface oxidation treatment. In comparison with other studies [10,23,24], our method has the following advantages. It provides a simple, environmental friendly and high-output way to generate stiff shells on the microspheres and simultaneously trigger surface wrinkling. Moreover, no external stimuli (e.g., stretching/compressing, solvent swelling, and heating) should be applied in our method, indicative of low equipment investment for large-scale preparation. Our study not only presents a simply, efficient and environmentally friendly method to fabricate microspheres with wrinkling surface morphologies, but also provides new insights into the wrinkling behavior on spherical surfaces by triggering interfacial instabilities.

2. Materials and methods

2.1. Materials

The PDMS precursors (Sylgard 184), including the base and curing agent, were purchased from Dow Corning Corporation. The non-ionic surfactants (Triton X-100 with a cloud point of 66 °C and Tween-20 with a cloud point beyond 100 °C) and the ionic surfactant (sodium dodecyl benzene sulfonate (SDBS)) were purchased from Haihong chemical Co., LTD, Chengdu.

2.2. Synthesis of PDMS microspheres

In procedure I, the PDMS base was mixed with the curing agent thoroughly in different base/curing agent weight ratio, *i.e.* 5:1, 10:1, 15:1, and 30:1. These PDMS base/curing agent mixtures were degassed for 25 min before use. The surfactant Triton X-100 was dissolved in deionized water with designed concentration, *i.e.* 0.7 wt%, 1 wt %,1.5 wt%, 3 wt%, 5 wt%, and 7.5 wt%. In procedure II, equal volumes of aqueous surfactant solution and PDMS base/curing agent mixture were mixed and stirred at room temperature for 2 h to form a stable emulsion. In procedure III, the PDMS droplets in the emulsion were cured at different temperatures (25 °C/48 h, 50 °C/12 h and 70 °C/12 h) with mechanical agitation. In procedure IV, the PDMS microspheres were dried by different methods (*i.e.* freeze-drying, hot-air-drying and hot-air-drying-after-filtrating) at varying temperatures (25 °C, 50 °C and, 70 °C). For conciseness, $PDMS_{(n:1)}$ microspheres represent the cured microspheres with a base/curing agent weight ratio of n:1. Control experiments were carried out using SDBS and Tween 20 as surfactants at a fixed concentration of 3 wt% under 50 °C. The resulting PDMS microspheres were dried with hot air drying process (Supporting Information, Fig. S6). And as-prepared PDMS microspheres were used directly.

2.3. Characterization

The surface morphologies of the PDMS microspheres were observed using a FEI Inspect F field-emission scanning electron microscope (SEM, Inspect F, FEI Company, USA). In order to improve the sample conductivity for SEM observation, the Au film were sputtered on the samples with an E-1045 ion sputter (HITACHI, Japan) at the sputtering rate of 3 nm/min under the pressure of 7 Pa and the current of 15 mA for 2 min at room temperature, and the thickness of the sputtered Au film is about 6 nm.

3. Results

The PDMS microspheres were synthesized in a conventional oil/water system, where the thermo-curable PDMS precursors (composed of curable PDMS and curing agent) were mixed with deionized water containing surfactants. The PDMS precursors were divided into small emulsion droplets in water with the aid of mechanical stirring and stabilized by surfactants [26–28]. The emulsion droplets were polydisperse in size which could be controlled by varying the oil/water ratio and/or surfactant concentration.

Fig. 1 shows the SEM images of the $PDMS_{(10:1)}$ microspheres prepared at various surfactant concentrations. These $PDMS_{(10:1)}$ microspheres had a wide size distribution (Fig. 1a). Compared to PDMS microbeads synthesized by microfluidic approaches [29], the polydispersity of our PDMS microspheres was relatively large. This wide radius distribution provided a good platform for simultaneous investigation of the influence of the microsphere size on the surface morphology of microspheres. As can be seen in Fig. 1c-g, the wrinkling patterns were generated on the microspheres over a large range of surfactant concentration (from 1 wt% to 7.5 wt%). The enlarged SEM images clearly demonstrated that these surfaces show labyrinth patterns (Fig. 1c-g (Inset)). For the microspheres prepared at a low surfactant concentration (0.7 wt%, Fig. 1b), it had a slightly wrinkled surface (or local wrinkled surface), this implies that the surfactant concentration plays a vital role in determining the formation of wrinkling patterns on microspheres. Another interesting finding is that the characteristic wavelength (λ) of the periodic wrinkles was independent of the surfactant concentration (φ) (Fig. 1 h).

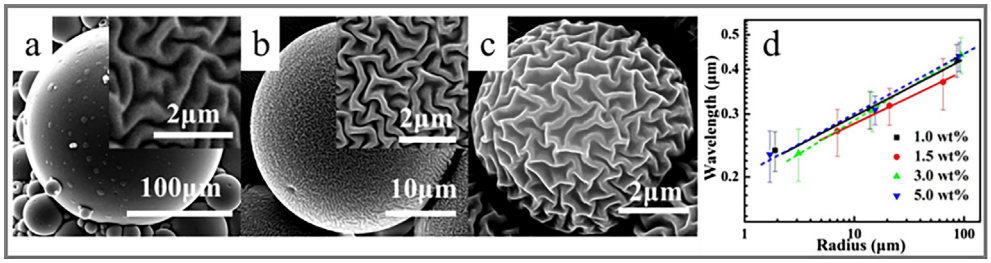

Fig. 2. Scanning electron microscope images of the wrinkling surface of microspheres with different diameters at surfactant concentration of 3 wt%.(Inset) At higher magnification. Frame d shows the λ ~ R relationship for $PDMS_{(10:1)}$microspheres with varying surfactant concentrations.

The wrinkling patterns of the $PDMS_{(10:1)}$ microspheres with different diameters at 3 wt% surfactant were shown in Fig. 2a–c. It can be found that the pattern ordering (labyrinth pattern) was nearly independent of the radius (*R*) of the PDMS microspheres. However, the characteristic wavelength increased linearly with the radius in the double-logarithmic plot (Fig. 2d). Here the wrinkling wavelength λ was estimated based on the SEM images (Figs. 2 and S1). We also found that there was no pattern generated on the surface of the very small microspheres (Fig. S2). Furthermore, Fig. 2d also showed that PDMS microspheres with the same radius but different surfactant concentration had similar wrinkling wavelength, consistent with the result of Fig. 1h. This further suggested that the surfactant concentration had little effect on the wrinkling wavelength of PDMS microspheres. In a word, the wrinkling wavelength was a function of the radius (*R*) of the PDMS microspheres but not the surfactant concentration.

The influence of the curing temperature on the wrinkling patterns of $PDMS_{(10:1)}$ microspheres was also investigated, see Fig. 3. Evidently, the wrinkling patterns only formed on the PDMS microspheres at low curing temperatures, *i.e.* at ambient temperature (Fig. 3a–c) and 50 °C (Fig. 3d–f, Fig. S3). At a higher curing temperature of 70 °C, no wrinkling pattern was observed (Fig. 3g–I, Fig. S4). Another interesting finding was that the small PMDS microspheres showed buckball-like pattern (Fig. 3f) rather than labyrinth pattern (e.g., see Fig. 3d and e) when the curing temperature was 50 °C.

The drying method was another factor influencing the wrinkling pattern on the PDMS microspheres. Very different textured surfaces were obtained with varying drying processes, see Fig. 4. For the large microsphere, the labyrinth pattern generated on microspheres when the hot-air-drying process and hot-air-drying-after-filtrating process were adopted (Fig. 4a and b). However, when the freeze-drying process was adopted, the smaller wavelength features were produced inside the larger wavelength ones on the microspheres (Fig. 4c), *i.e.* hierarchical wrinkling [30,31]. For the small microspheres (Fig. 4d–f), the labyrinth pattern was formed with the hot-air-drying process, while the buckball-

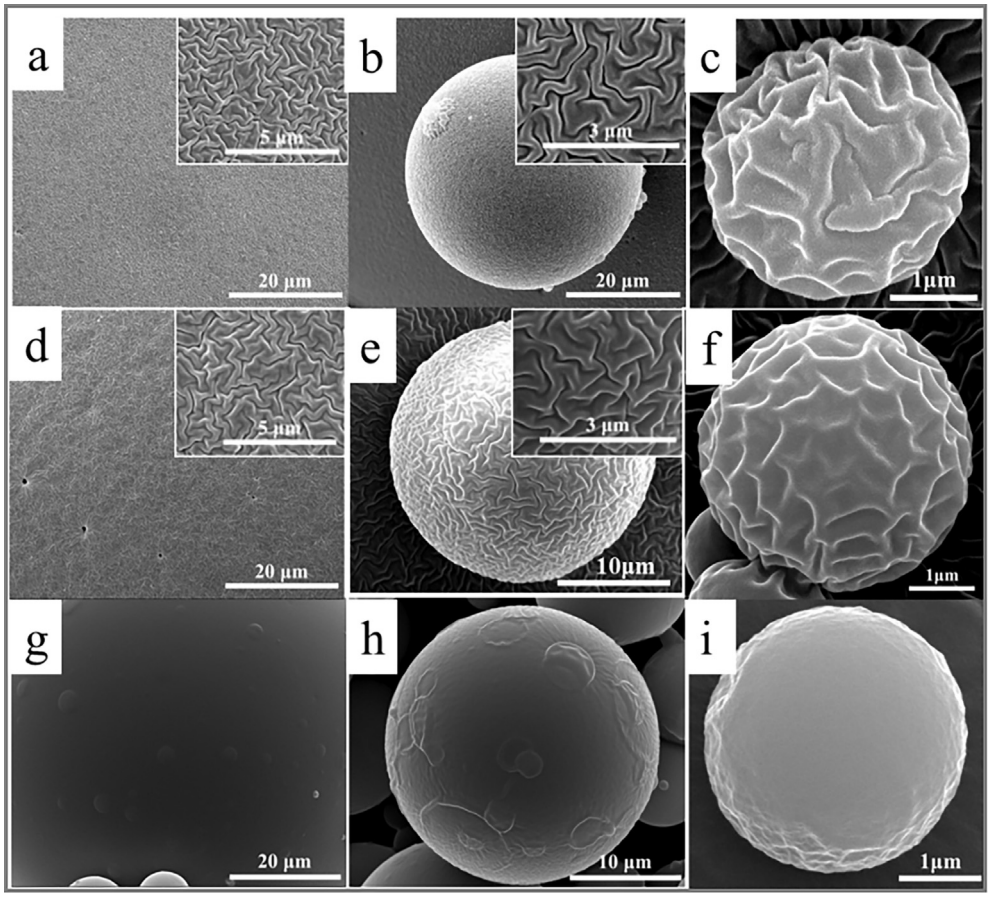

Fig. 3. Scanning electron microscope images of the varisized microspheres (3 wt% surfactant, hot air drying after filtrating) with varying curing temperature, (a–c) 25 °C; (d–f) 50 °C; (g–i) 70 °C. (Inset) At higher magnification.

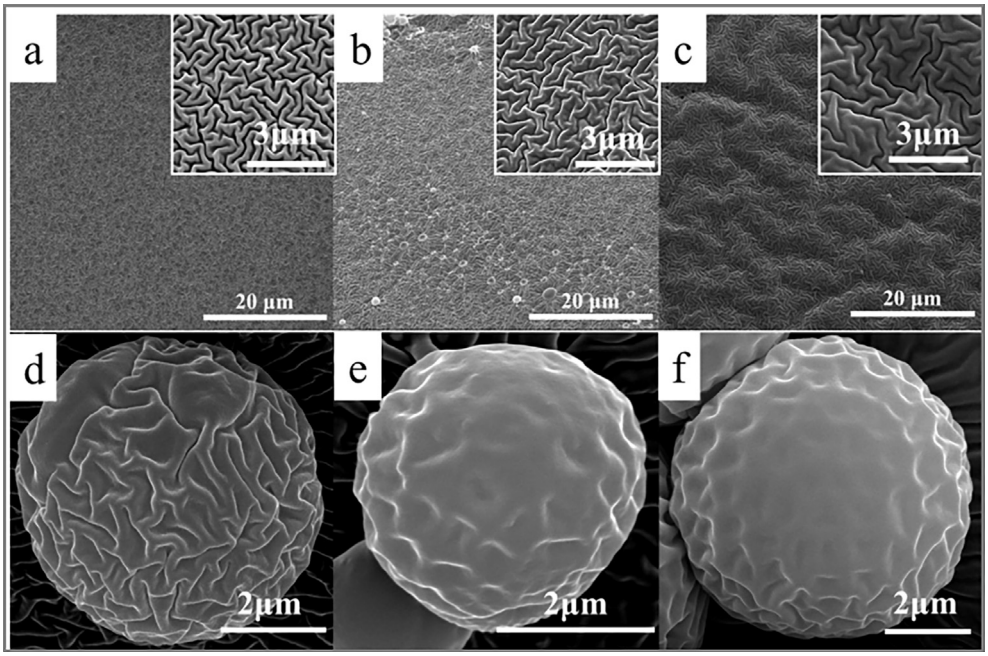

Fig. 4. Scanning electron microscope images of varisized microspheres (3 wt% surfactant, curing temperature 50 °C) with varying drying methods. (a, d) hot air drying (50 °C, 12 h); (b, e) hot air drying after filtrating (50 °C, 12 h); (c, f) freeze-drying (−50 °C, 24 h, ~10 Pa). (Inset) at high magnification.

like patterns were generated with the hot-air-drying-after-filtrating process and freeze-drying process. Moreover, the influence of the curing time and Young's modulus of $PDMS_{(n:1)}$ microspheres ($E_{PDMS(n:1)}$) on the surface wrinkling behavior have also been investigated (Figs. S5 and S7). The labyrinth patterns and dimples formed on the large PDMS microspheres and small PDMS microspheres, respectively (Fig. S5), and the wrinkling patterns have no dependence of curing time.

The surface wrinkling patterns on the microspheres changes from the smooth surface, labyrinths to the dimples with the decreasing Young's modulus of PDMS microspheres (Fig. S7).

The above results indicated that it is possible to tune the wrinkling patterns on the PDMS microspheres by changing the surfactant concentration, curing temperature and drying methods. The mechanism of forming the wrinkling patterns on the PDMS microspheres will be discussed in detail below.

4. Discussions

It is well known that wrinkling occurs in thin film/substrate systems when the compressive stress σ between the thin film and substrate is higher than the critical threshold σ_c. Depending on the physical properties of the thin film and substrate and by assuming a sinusoidal waveform of the generated buckling instability, the critical stress σ_c and the wavelength of buckling (λ) can be expressed by [32,33]:

$$\sigma_c = \frac{\bar{E}_f}{4}\left(\frac{3\bar{E}_s}{\bar{E}_f}\right)^{2/3} \tag{1}$$

$$\lambda = 2\pi h\left(\frac{\bar{E}_f}{3\bar{E}_s}\right)^{1/3} \tag{2}$$

where h is the film thickness, $\bar{E}$ is the plane-strain modulus, defined as $E/(1-\nu^2)$ with E being the Young's modulus and ν being the Poisson's ratio. The subscripts f and s represent film and substrate, respectively.

However, the geometrical constraint engenders apparently different wrinkling behaviors on a curved surface from those on a planar surface [16–19]. Cao and Yin et al. [16] utilized the finite element method (FEM) to investigate the correlation of the wrinkling patterns with the normalized substrate radius of curvature R/h and the overstress σ^R/σ_c^R in a spherical Ag core/SiO_2 shell system. Here σ^R and σ_c^R refer to the applied stress and the critical wrinkling stress on a spherical core/shell system with the shell thickness h and the substrate radius R, respectively. Then σ_c^R can be determined by:

$$\frac{\sigma_c^R}{\sigma_c} \approx 1 + \Omega^2 \tag{3}$$

where Ω is the introduced dimensionless curvature parameter [23], which is defined as:

$$\Omega = 2\sqrt{(1-\nu_f^2)}\,(h/R)\left(\frac{\bar{E}_f}{3\bar{E}_s}\right)^{2/3} \tag{4}$$

According to the equations, it is seen that σ_c^R is intimately dependent on the h/R and $\bar{E}_f/\bar{E}_s$. Meanwhile, Cao's spherical model results reveal the following scaling relation between the wrinkling wavelength λ and R/h

$$\frac{\lambda}{R} = a\left(\frac{R}{h}\right)^b \tag{5}$$

where a and b are two fitting parameters. Furthermore, in the work of Cao et al., a and b are 3.0 and −0.8, respectively [16]. Then it can be simplified as:

$$\lg\lambda = 0.2\lg R + C \tag{6}$$

where C is a constant. From the experimental result of Yin et al. [25] on the PDMS microspheres with spherical wrinkles initiated by surface chemical oxidization in a strong acid mixture, the obtained λ and R approximately satisfied:

$$\lg\lambda = 0.3\lg R - 0.33 \tag{7}$$

In the current case (*i.e.* 3 wt% surfactant, curing temperature 25 °C and hot air drying 50 °C), according to the results presented in Fig. 2d, λ and R approximately satisfied the following linear relation:

$$\lg\lambda = 0.19\lg R - 0.73 \tag{8}$$

Apparently, the slope in Eq. (8) was comparable to those given in Eqs. (6) and (7). Therefore, it is probably that the PDMS microspheres in our system also have a core-shell structure as shown in Scheme 1a. An interfacial layer, containing PDMS chains, H_2O and surfactant, was

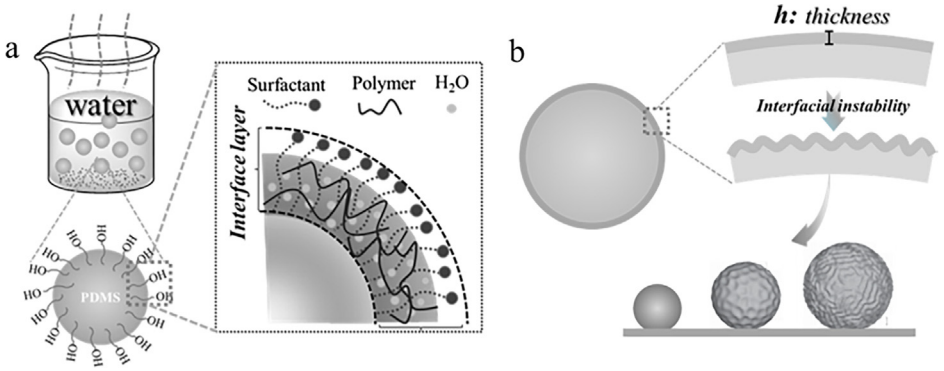

Scheme 1. (a) Schematic diagram for the interface layer formation at the oil/water interface, (b) illustration of the formation of buckling patterns, which triggered by the interfacial instability of interface layer during the curing and drying process.

formed at the oil/water interface of droplets. We propose that by curing the PDMS droplets and then drying the interfacial layer, the interfacial instabilities were triggered and the buckling patterns were generated on the surface of PDMS microspheres, as presented in Scheme 1b. For small microspheres (Fig. S2), the critical stress for buckling may become too large (scaled with h/R, see Eq. (4), leading to the disappearance of wrinkling patterns [24,34]. The slight difference among the slope values can be ascribed to the different wrinkling systems and the corresponding experimental conditions [16,22]. Additionally, this deviation from theoretical predictions might be due to the fact that the interfacial layer has a compressive stress gradient rather than a constant compressive stress distribution which usually assumed in the theoretical work [35–37].

According to Eqs. (1)–(5), it is known that the shell thickness h, microsphere radius R and $\bar{E}_f/\bar{E}_s$have important effects on the dimensionless curvature parameter Ω, the critical wrinkling stress σ_c^R, the overstress σ^R/σ_c^R, and the resulting wrinkling morphologies. Based on our results, the variation of wrinkling patterns had been found on the small microspheres with varying experimental conditions. This is ascribed to the highly sensitive excess stress at small radius [23].

On the basis of the aforementioned theories and our experimental results, we propose that the wrinkling surface patterns are influenced by the variation of thickness of interfacical layer (shell layer) under the varying experimental conditions as displayed in Scheme 2. It is well accepted that the packing density of surfactants on the surface of emulsion droplets increases with surfactant concentration and then keeps constant at high surfactant concentrations. The adsorption of surfactant has a positive effect on the thickness of interfacial layer. Therefore, the thickness of interface layer increases with surfactant concentration and then keeps constant (Scheme 2a), leading to the corresponding changes of wrinkling patterns (*i.e.* from smooth surfaces to wrinkling surfaces, see Fig. 1). As we all know, not only the activity and diffusion rate of surfactant but also the spherical substrate modulus are affected by the curing temperature. And the spherical substrate modulus increases with the curing temperature. Combined with the results in Fig. S7, it can be concluded that the activity and diffusion rate of surfactant is the dominant factor for the change of wrinkling patterns. Below the cloud point the activity and diffusion rate of surfactant increase with increasing temperature, while close to or above the cloud point the nonionic surfactant would deactivate and aggregate [38,39]. The activity and diffusion rate of surfactant play important roles in determining the thickness of interfacial layer. As a result, when the curing temperature is 25 °C and 50 °C (below the cloud point, 66 °C for Triton X-100), the thickness of interfacial layer increases with temperature due to the increasing of activity and diffusion rate of surfactant, and when the curing temperature is above the cloud point, the thickness of interface starts to decrease due to the deactivate and aggregate of surfactant (Scheme 2b). The corresponding wrinkling morphology changes from the labyrinth pattern to the buckyball-like pattern and then to a smooth surface as shown in Fig. 3. Regarding to the drying process of the PDMS microspheres, the interfacial layer undergoes different relaxation behaviors under different drying process, which play a crucial role in the surface morphology of the microspheres. When freeze drying, a technique to improve the long-term stability of colloids, was adopted [40], the configuration of PDMS microspheres was well maintained, resulting in little decrease in interfacial layer thickness (Scheme 2c). Regarding hierarchical structure generation in a previous study, [30] the accumulated thermal stress in the confined geometry of the metal/polymer bilayer system is slowly released via a wrinkling process in which a double scale wrinkling takes place depending on the relaxation mode of the confined polymeric layer. Therefore, we supposed that the double-scale wrinkling wavelength generation is ascribed to the relaxation mode of the confined interfacial layer during the freeze-drying process. During the hot-air-drying process, *i.e.* the slowest drying process in our study, the interfacial layer of PDMS microspheres had relaxed for a long time, resulting in a sharply decrease in its thickness (Scheme 2c). As the thickness decreases with the time of relaxation (η), the wrinkling patterns change from labyrinth (by hot-air-drying process) to the buckball-like pattern (by hot-air-drying-after-filtrating and freeze-drying process) (Fig. 4).

According to the proposed mechanism in Scheme 2, it can be expected that reversible switch between the highly textured surface and the smooth surface could be realized through water swelling and drying. Indeed, this is observed in our experiments. As depicted in Fig. 5, when dried PDMS microspheres were immersed in water, the primary labyrinth and buckball-like patterns (Fig. 5a and d) transformed into smooth surfaces (Fig. 5b and e). When the water-swollen system dried out again, the highly textured patterns (Fig. 5c and f) were re-formed on the surface of microsphere with negligible changes. This phenomenon revealed that the wrinkles formed during drying process. The sustainable transformation of the surface morphologies of the PDMS microspheres through simple wetting/drying processes could extend their practical applications and enable their use as sensors, responsive coating and microfluidic devices.

5. Conclusions

In summary, the PDMS microspheres with controllable surface wrinkling patterns, including labyrinth and buckyball-like, were obtained from a conventional oil/water emulsion system with surfactants. It is found that the wrinkling wavelength λ and the microsphere radius R have the power-law dependency, which is in agreement with a theoretical model proposed for spherical core/shell system. The resultant stable wrinkling morphologies are sensitive to the substrate radius of curvature R/h and overstress σ^R/σ_c^R. Here, R/h and σ^R/σ_c^R have been well tuned by the experimental conditions such as the surfactant concentration, curing temperature, evaporation rate and weight ratio between base and curing agent. Additionally, the microspheres could be

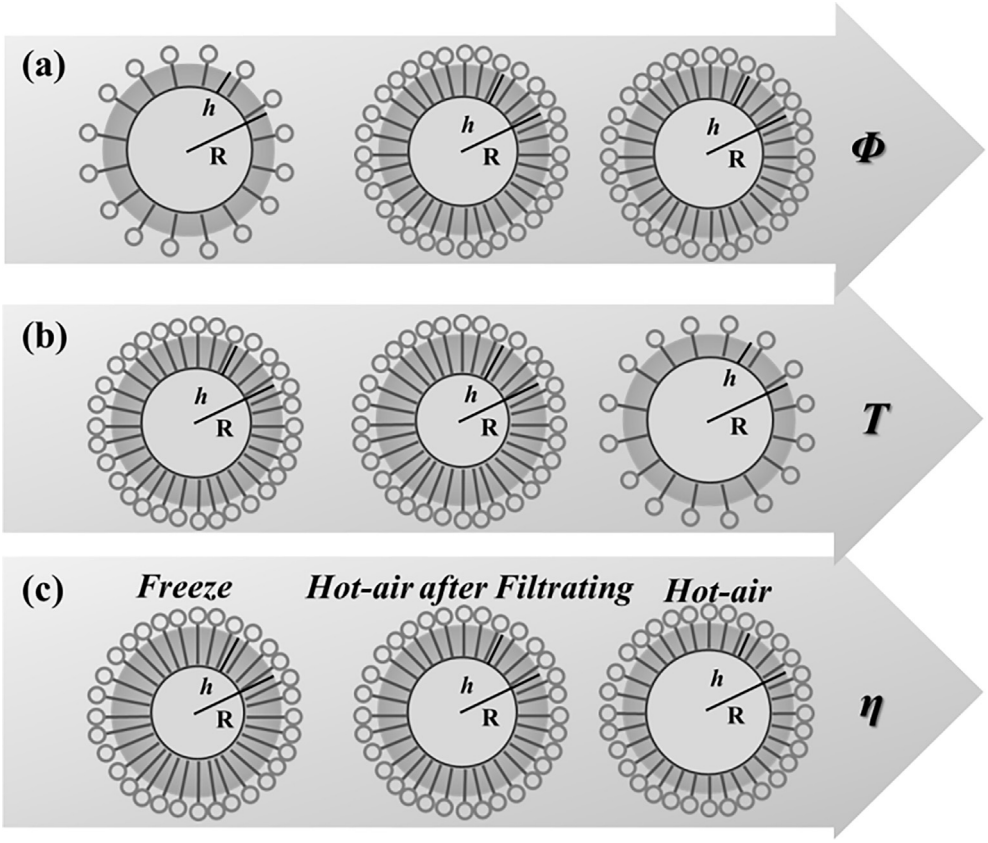

Scheme 2. The schematic illustration of the evolution of the thickness of interface layer with varying experimental conditions, (a) surfactant concentration, (b) curing temperature, (c) drying method.

reversibly switched between the wrinkling patterns and the no-pattern surface simply by wetting with water and drying. These tunable surfaces have potential for preparing new functional surfaces. It seems that evaporation of water in the interfacial layer on the PDMS microspheres triggers the interfacial instabilities and therefore the formation of surface wrinkling patterns.

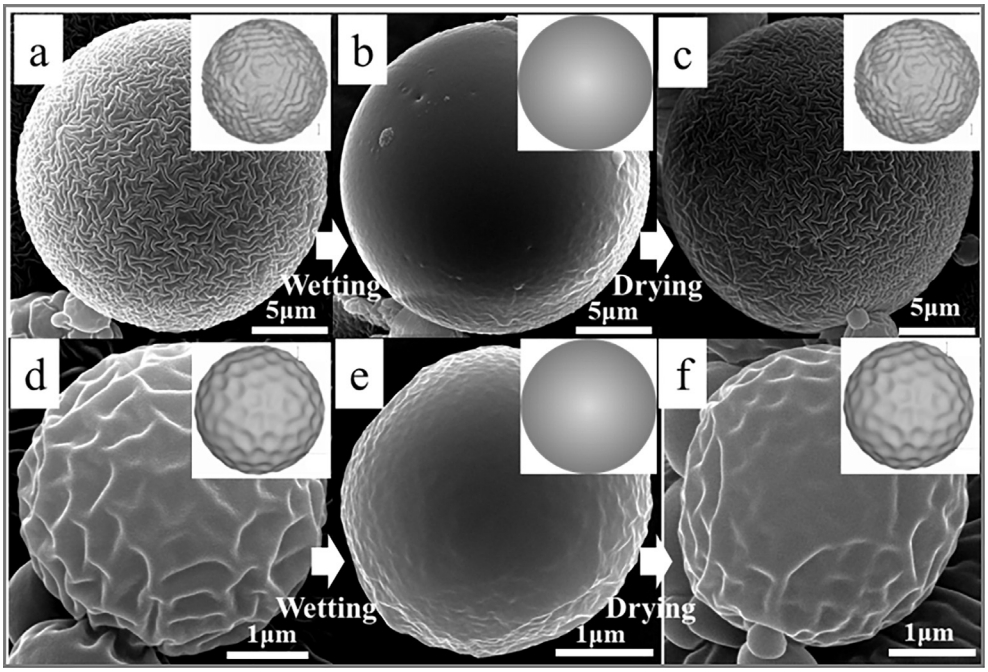

Fig. 5. Scanning electron microscope images of the winkling surface of varisized microspheres (3 wt% surfactant, curing temperature 50 °C) for the revisable behavior by an ex-situ wetting-redrying process. (a, d) the original dried microspheres; (b, e) the wetted microspheres; (c, f) the re-dried microspheres.

Acknowledgements

This research was supported by the National Natural Science Foundation of China (Grant No. 21674069, 51422305).

Appendix A. Supplementary material

Supplementary data associated with this article can be found, in the online version, at https://doi.org/10.1016/j.eurpolymj.2018.05.007.

References

[1] E. Schaffer, T. Thurn-Albrecht, T.P. Russell, U. Steiner, Electrically induced structure formation and pattern transfer, Nature 403 (6772) (2000) 874–877.
[2] T. Thorsen, R.W. Roberts, F.H. Arnold, S.R. Quake, Dynamic pattern formation in a vesicle-generating microfluidic device, Phys. Rev. Lett. 86 (18) (2001) 4163–4166.
[3] D.P. Holmes, A.J. Crosby, Snapping surfaces, Adv. Mater. 19 (21) (2007) 3589–3593.
[4] A. Sidorenko, T. Krupenkin, A. Taylor, P. Fratzl, J. Aizenberg, Reversible switching of hydrogel-actuated nanostructures into complex micropatterns, Science 315 (5811) (2007) 487–490.
[5] S. Shian, D.R. Clarke, Electrically tunable window device, Opt. Lett. 41 (6) (2016) 1289–1292.
[6] E.P. Chan, A.J. Crosby, Fabricating microlens arrays by surface wrinkling, Adv. Mater. 18 (24) (2006) 3238–3242.
[7] B. Bao, J. Jiang, F. Li, P. Zhang, S. Chen, Q. Yang, et al., Fabrication of patterned concave microstructures by inkjet imprinting, Adv. Funct. Mater. 25 (22) (2015) 3286–3294.
[8] B. Bao, J. Sun, M. Gao, X. Zhang, L. Jiang, Y. Song, Patterning liquids on inkjet-imprinted surfaces with highly adhesive superhydrophobicity, Nanoscale 8 (18) (2016) 9556–9562.
[9] J. Sun, J. Jiang, B. Bao, S. Wang, M. He, X. Zhang, et al., Fabrication of bendable circuits on a polydimethylsiloxane (PDMS) surface by inkjet printing semi-wrapped structures, Materials 9 (4) (2016) 253.
[10] Y. Jeong, Y.-C. Chen, M.K. Turksoy, S. Rana, G.Y. Tonga, B. Creran, A. Sanyal, A.J. Crosby, V.M. Rotello, Tunable elastic modulus of nanoparticle monolayer films by host-guest chemistry, Adv. Mater. 26 (29) (2014) 5056–5061.
[11] C.M. Stafford, C. Harrison, K.L. Beers, A. Karim, E.J. Amis, M.R. VanLandingham, H.-C. Kim, W. Volksen, R.D. Miller, E.E. Simonyi, A buckling-based metrology for measuring the elastic moduli of polymeric thin films, Nat. Mater. 3 (8) (2004) 545–550.
[12] M. Guvendiren, S. Yang, J.A. Burdick, Swelling-induced surface patterns in hydrogels with gradient crosslinking density, Adv. Funct. Mater. 19 (19) (2009) 3038–3045.
[13] N. Bowden, S. Brittain, A.G. Evans, J.W. Hutchinson, G.M. Whitesides, Spontaneous formation of ordered structures in thin films of metals supported on an elastomeric polymer, Nature 393 (6681) (1998) 146–149.
[14] J. Genzer, J. Groenewold, Soft matter with hard skin: From skin wrinkles to templating and material characterization, Soft Matter 2 (4) (2006) 310–323.
[15] J. Yin, X. Chen, I. Sheinman, Anisotropic buckling patterns in spheroidal film/substrate systems and their implications in some natural and biological systems, J. Mech. Phys. Solids 57 (9) (2009) 1470–1484.
[16] G. Cao, X. Chen, C. Li, A. Ji, Z. Cao, Self-assembled triangular and labyrinth buckling patterns of thin films on spherical substrates, Phys. Rev. Lett. 100 (3) (2008) 036102.
[17] B. Li, Y.-P. Cao, X.-Q. Feng, H. Gao, Mechanics of morphological instabilities and surface wrinkling in soft materials: a review, Soft Matter 8 (21) (2012) 5728–5745.
[18] J. Yin, Z. Cao, C. Li, I. Sheinman, X. Chen, Stress-driven buckling patterns in spheroidal core/shell structures, Proc. Natl. Acad. Sci. 105 (49) (2008) 19132–19135.
[19] X. Chen, J. Yin, Buckling patterns of thin films on curved compliant substrates with applications to morphogenesis and three-dimensional micro-fabrication, Soft Matter 6 (22) (2010) 5667–5680.
[20] N. Stoop, R. Lagrange, D. Terwagne, P.M. Reis, J. Dunkel, Curvature-induced symmetry breaking determines elastic surface patterns, Nat. Mater. 14 (3) (2015) 337–342.
[21] B. Li, F. Jia, Y.-P. Cao, X.-Q. Feng, H. Gao, Surface wrinkling patterns on a core-shell soft sphere, Phys. Rev. Lett. 106 (23) (2011) 234301.
[22] A.C. Trindade, J.P. Canejo, L.F.V. Pinto, P. Patrício, P. Brogueira, P.I.C. Teixeira, M.H. Godinho, Wrinkling labyrinth patterns on elastomeric Janus particles, Macromolecules 44 (7) (2011) 2220–2228.
[23] Q. Li, X. Han, J. Hou, J. Yin, S. Jiang, C. Lu, Patterning poly(dimethylsiloxane) microspheres via combination of oxygen plasma exposure and solvent treatment, J. Phys. Chem. B 119 (42) (2015) 13450–13461.
[24] D. Breid, A.J. Crosby, Curvature-controlled wrinkle morphologies, Soft Matter 9 (13) (2013) 3624–3630.
[25] J. Yin, X. Han, Y. Cao, C. Lu, Surface wrinkling on polydimethylsiloxane microspheres via wet surface chemical oxidation, Sci. Rep. 4 (2014) 5710.
[26] L. González, M. Baoguang, L. Li, J.H. Hansen, S. Hvilsted, A.L. Skov, Encapsulated PDMS microspheres with reactive handles, Macromol. Mater. Eng. 299 (6) (2014) 729–738.
[27] B. Ma, J.H. Hansen, S. Hvilsted, A.L. Skov, Investigation into accessible surface vinyl concentrations of nonstoichiometric PDMS microspheres from hydrosilylation reactions and their further crosslinking reactions, Macromol. Mater. Eng. 300 (6) (2015) 627–636.
[28] S. Liu, R. Deng, W. Li, J. Zhu, Polymer microparticles with controllable surface textures generated through interfacial instabilities of emulsion droplets, Adv. Funct. Mater. 22 (8) (2012) 1692–1697.
[29] K. Jiang, P.C. Thomas, S.P. Forry, D.L. DeVoe, S.R. Raghavan, Microfluidic synthesis of monodisperse PDMS microbeads as discrete oxygen sensors, Soft Matter 8 (4) (2012) 923–926.
[30] P.J. Yoo, H.H. Lee, Evolution of a stress-driven pattern in thin bilayer films: spinodal wrinkling, Phys. Rev. Lett. 91 (15) (2003) 154502.
[31] J.-Y. Park, H.Y. Chae, C.-H. Chung, S.J. Sim, J. Park, H.H. Lee, et al., Controlled wavelength reduction in surface wrinkling of poly(dimethylsiloxane), Soft Matter 6 (3) (2010) 677–684.
[32] H. Jiang, D.-Y. Khang, J. Song, Y. Sun, Y. Huang, J.A. Rogers, Finite deformation mechanics in buckled thin films on compliant supports, Proc. Natl. Acad. Sci. 104 (40) (2007) 15607–15612.
[33] S. Yang, K. Khare, P.-C. Lin, Harnessing surface wrinkle patterns in soft matter, Adv. Funct. Mater. 20 (16) (2010) 2550–2564.
[34] S. Cai, D. Breid, A.J. Crosby, Z. Suo, J.W. Hutchinson, Periodic patterns and energy states of buckled films on compliant substrates, J. Mech. Phys. Solids 59 (5) (2011) 1094–1114.
[35] M. Nania, O.K. Matar, J.T. Cabral, Frontal vitrification of PDMS using air plasma and consequences for surface wrinkling, Soft Matter 11 (15) (2015) 3067–3075.
[36] B.A. Glatz, M. Tebbe, B. Kaoui, R. Aichele, C. Kuttner, A.E. Schedl, H.-W. Schmidt, W. Zimmermann, A. Fery, Hierarchical line-defect patterns in wrinkled surfaces, Soft Matter 11 (17) (2015) 3332–3339.
[37] Y. Yang, X. Han, W. Ding, S. Jiang, Y. Cao, C. Lu, Controlled free edge effects in surface wrinkling via combination of external straining and Selective O2 plasma exposure, Langmuir 29 (23) (2013) 7170–7177.
[38] K. Shinoda, H. Saito, The effect of temperature on the phase equilibria and the types of dispersions of the ternary system composed of water, cyclohexane, and nonionic surfactant, J. Colloid Interface Sci. 26 (1) (1968) 70–74.
[39] K. Shinoda, H. Saito, The Stability of O/W type emulsions as functions of temperature and the HLB of emulsifiers: the emulsification by PIT-method, J. Colloid Interface Sci. 30 (2) (1969) 258–263.
[40] W. Abdelwahed, G. Degobert, S. Stainmesse, H. Fessi, Freeze-drying of nanoparticles: formulation, process and storage considerations, Adv. Drug Deliv. Rev. 58 (15) (2006) 1688–1713.